Skin and Ophthalmic Tissue Disposition of Topically Applied Drugs on Eyelid Skin: Optimization of Drug Targeting to Conjunctiva and Eyeball

(Draft)

2019

Gerard Lee Lo See

General Introduction

For several years, ophthalmic drug dosage forms remain one of the paramount and extensively developed areas of pharmaceutical technology. The predicament of low bioavailability of medicinal substance after application to the eyeball is the foremost reason of scientists' continuingly strong interest in search for better methods for ophthalmic drug delivery.

Current methods of delivering medicines to the eyes includes topical, oral, and parenteral routes. These preparations offer benefit of high patient compliance, self-administrable, and evade blood-retinal barrier, respectively. Despite the various benefits of these preparations, several drawbacks are associated with the current dosage forms. Eye drops have poor bioavailability because of dilution and excretion by tear fluid. Ophthalmic medicines taken orally have little to no efficacy due to first-pass metabolism before reaching the eye biophase. Moreover, parenteral route of administration requires clinical support by ophthalmologists and decreases patient convenience due to frequent visitation in medical facility and consequently reduces patient compliance. There is a need to search for an alternative method to deliver drugs into the eyes to improve low bioavailability of medicines in the eyes.

The skin provides an alternative route for drug administration allowing sustained drug delivery to the blood circulatory system, providing greater patient comfort while avoiding several side effects of oral, topical and parenteral administration. Transdermal delivery for the eyes can maintain a constant blood concentration for a long duration. The major goal of ophthalmic drug delivery is attainment and retention at the site of action within the eye.

Eyelid skin, the thinnest skin layer (<1mm) in the body, offers an alternative site to deliver drugs into the eyes. A unique feature of eyelids from the drug delivery standpoint is their proximity to the conjunctiva, which is between 2 and 30 times more permeable to drugs

than cornea. It must be noted that the conjunctiva has a direct contact with the eyeball and its surrounding ocular tissues. With the presence of drugs in the conjunctiva, it is expected to distribute into the anterior and posterior ocular regions, the delivery target area in most ocular diseases. Given the limited number of studies investigating the delivery of drugs into the conjunctiva and eyeball through eyelid skin and the paucity of data describing eyelid drug permeation, this prompted us to conduct the following studies. In Chapter 1, we established the potential of the eyelid skin for the delivery of drugs in the conjunctiva and ocular tissues. In Chapter 2, we investigated the effect of adding physical methods, iontophoresis, to promote percutaneous absorption of drugs into the eyeball through the eyelid skin. In Chapter 3, we investigated the ocular tissue distribution and pharmacokinetic profile of drugs delivered via eyelid skin.

Chapter 1

Eyelid skin as a potential site for drug delivery to conjunctiva and ocular tissues

1.1 Introduction

For several decades, eye drops remain one of the paramount and extensively utilized pharmaceutical formulations for various ocular diseases (i.e., eyeball and surrounding tissues) (Baranowski et al., 2014). Currently, the eye drops account for about 90% of ophthalmic medicines primarily due to ease of administration and good patient compliance. However, several drawbacks are associated with the utilization of eye drops. Eye medications cannot be administered beyond the capacity of the conjunctival sac due to its limited volume. Most eye drops exhibit low bioavailability, poor targeting efficacy, and virtually impossible to administer during sleep. Anatomical and physiological constrains such as tear turnover, nasolacrimal drainage, reflex blinking, and ocular static and dynamic barriers impede the bioavailability and controlled delivery of drugs administered as eye drops (Kimura et al., 2007; Gaudana et al., 2010; Isowaki et al., 2003; Gause et al., 2015). With these impediments, it is essential to search for an alternative approach to deliver ophthalmic drugs with high targeting ability while simultaneously improving drug absorption into the ocular tissues.

We then paid attention to applying and delivering ophthalmic drugs on the (lower) eyelid skin using various forms of formulations. The lower eyelid skin exhibits less movement due to blinks as compared to upper eyelid skin making it a good site for administration. Moreover, it is very interesting for skin researchers to explore the eyelids, the thinnest skin layer among the human body (< 1 mm) (Amirlak and Sahshabi, 2015). Generally, the thinner the stratum corneum, the greater the drug permeation. In addition, drug administration through the skin

provides several advantages as it generally facilitates avoidance of premature metabolism, decreased toxicity, fewer side effects as well as greater patient compliance (Paudel et al., 2010).

A unique feature of eyelids from the drug delivery standpoint is their proximity to the conjunctiva, which is between 2 and 30 times more permeable to drugs than cornea (Davies, 2000). It must be noted that the conjunctiva has a direct contact with the eyeball and its surrounding ocular tissues. With the presence of drugs in the conjunctiva, it is expected to distribute into the anterior and posterior ocular regions, the delivery target area in most ocular diseases. In addition, transdermal drug delivery could maintain a constant drug concentration in the dermal layers beneath the application site for a longer duration. This is the most beneficial point compared with eye drops application, which has many drawbacks, as described above. If drugs could be delivered to the conjunctival tissue via the eyelid skin, these drawbacks associated with the eye drops could be addressed. Moreover, once medications are prepared for eyelid administration, greater convenience is obtained for patients with ocular diseases (i.e., allergic conjunctivitis, eye infections, glaucoma) and health care professionals alike. Time for drug administration by patients or health care professionals is reduced while treatment may continue albeit the patient is asleep thereby increasing drug retention time and consequently improving patient comfort and quality of life.

Given the limited number of studies investigating the delivery of drugs into the conjunctiva through eyelid skin and the paucity of data describing eyelid drug permeation, it prompted us to study hydrophilic and lipophilic model compounds and to compare permeability characteristics through the eyelid and the abdominal skin. In the present study, the researchers selected hairless rats as model animal, since it is more practical to conduct *in vivo* and *in vitro* experiments compared to other larger animal models. The researchers believe that this study for ophthalmic drug delivery utilizing rat eyelid skin was conducted for the first time. Pilocarpine hydrochloride, tranilast, antipyrine, diclofenac sodium, aminopyrine and lidocaine

were used to evaluate their skin permeation, former two were used to evaluate the skin concentration and two fluorescent dyes (fluorescein sodium and rhodamine B) were used to determine the *in vivo* distribution of the drugs in the conjunctiva.

1.2 Materials and Methods

1.2.1 Materials and Experimental Animals

Pilocarpine hydrochloride was purchased from Sigma-Aldrich (St. Louis, MO, USA). Lidocaine and tranilast were purchased from Tokyo Chemical Industry Co. Ltd. (Tokyo, Japan). Aminopyrine, antipyrine, diclofenac sodium, fluorescein sodium and rhodamine B were purchased from Wako Pure Chemical Industries, Ltd. (Osaka, Japan). Table 1 lists chemicals used as model permeants and their physicochemical properties.

Male hairless rats (WBM/ILA-Ht, 8 weeks of age, body weight of 220 – 260 g) were obtained from the Life Science Research Center, Josai University (Sakado, Saitama, Japan) or Ishikawa Experimental Animal Laboratories (Fukaya, Saitama, Japan). All animal feeding and experiments were approved by Institutional Animal Care and Use Committee of Josai University.

1.2.2 Preparation of Skin Membranes

Whole abdominal and (lower) eyelid skin were freshly excised from hairless rats previously shaved under three types of anesthesia (0.375 mg/kg medetomidine, 2.5 mg/kg butorphanol, 2 mg/kg midazolam) administered intraperitoneally. The excised skin was cleaned with pH 7.4 phosphate buffered saline (PBS).

1.2.3 Skin Permeation Experiments

Skin permeation experiments were carried out using Franz type vertical diffusion cells. Excess subcutaneous fat was trimmed off from the excised intact abdominal skin and no trimming was done for the eyelid skin. The eyelid skin was placed on a stabilizing apparatus with an effective diffusion area of 0.0707 cm^2 before it was set in a vertical diffusion cell. The abdominal skin sample was directly set in a vertical type diffusion cell with an effective diffusion area of 1.77 cm^2. One mL of PBS which corresponded to the donor solution and contained no permeant, was applied to the epidermis side and 6.0 mL of PBS was applied to dermis side of the skin to reach an equilibration state for about one hour. After an hour, the PBS of the epidermis side was replaced with the same volume of the donor solution (model compounds dissolved in PBS) to commence the permeation experiment. The receiver solution was stirred with a stirrer bar on a magnetic stirrer and maintained at 32°C using a thermostatically controlled heater throughout the experiments. An aliquot (500 μL) was withdrawn from the receiver chamber and the same volume of fresh PBS was added to the chamber to keep the volume constant. The penetrant concentration in the receiver chamber was determined by HPLC.

1.2.4 Determination of Skin Concentrations

The concentrations of the compounds in intact rat skin were measured 8 h after the start of the experiments, which were performed separately from the experiments mentioned above. The donor solution was removed, the stratum corneum side was rinsed three times with 1.0 mL of PBS and the compound-applied area was cut out. When the concentrations in viable epidermis and dermis were measured, the stratum corneum was removed by 20 times tape-stripping before clipping out the application area. The piece of skin was reduced in size using scissors and 0.5 mL of PBS was added prior to homogenization at 12,000 rpm and 4°C for 5 min using a homogenizer (Polytron PT 1200 E, Kinematica AG, Littaue-Lucerne,

Switzerland). For the deproteinization, 0.5 mL of 16% trichloroacetic acid in PBS was added to the skin homogenate, followed by agitation at 32°C for 15 min, and then the mixture was centrifuged at 15,000 rpm and 4°C for 5 min. The compound concentration in the resulting supernatant was determined by HPLC.

1.2.5 HPLC analysis

Samples were mixed with the same volume of acetonitrile containing the internal standard and centrifuged at 15,000 rpm and 4°C for 5 min. The obtained supernatant (20 μL) was injected into an HPLC system. The HPLC system (Shimadzu Co., Kyoto, Japan) consisted of a system controller (SCL-10A), pump (LC-20AD), degasser (DGU-20A_3), auto – injector (SIL-20A), column oven (CTO-20A), UV detector (SPD-20A) and analysis software (LC Solution). The column used was Inertsil® ODS-3 4.6 mm X 150 mm, 5μm (GL Sciences Inc., Tokyo, Japan). The column was maintained at 40°C and the flow rate of the mobile phase was adjusted to 1.0 mL/min. Refer to Table 2 for the details of the HPLC conditions.

Table 2. HPLC conditions for analysis of chemicals used in the study

Chemical	Mobile phase	Detection wavelength (nm)	Internal standard
Aminopyrine	Acetonitrile : 0.1% phosphoric acid containing 5 mM sodium dodecylsulphonate = 40 : 60	245	*p*-hydroxybenzoic acid methyl ester
Antipyrine	Acetonitrile : water = 20 : 80	254	---[a]
Diclofenac Na	Methanol : 0.1% phosphoric acid = 80 : 20	286	*p*-hydroxybenzoic acid ethyl ester
Lidocaine	Acetonitrile : 0.1% phosphoric acid containing 5mM 1-heptanesulphonate = 35 : 65	245	*p*-hydroxybenzoic acid n-propyl ester
Pilocarpine	Acetonitrile : 0.1% phosphoric acid= 5 : 95	212	---[a]
Tranilast	Acetonitrile : 0.1% phosphoric acid =40:60	230	*p*-hydroxybenzoic acid ethyl ester

[a] *Absolute calibration curve method was used*

1.2.6 Data analysis

The cumulative amount of model drugs permeated through the eyelid and the abdominal skin was calculated and expressed as the mean ± S.E. The permeation rate or flux (J, $\mu g/cm^2/h$), 6 to 8 h after starting the experiment, was determined based on the slope of linear regression of the cumulative amount of the model drugs against permeation time.

1.2.7 In vivo application study

In this part of the study, three hairless rats were used. The left eye was designated for the model compound to be delivered through a tube simulating transdermal drug delivery while the right eye was designated for the compound to be administered by drops simulating an eye drop. The rats were anesthetized with three types of anesthesia (0.375 mg/kg medetomidine, 2.5 mg/kg butorphanol, 2 mg/kg midazolam) administered intraperitoneally for the duration of the sampling period. A Teflon tube (internal diameter 3 mm) was glued on the left eyelid skin with cyanoacrylate bond (Aron Alpha, Konishi Co. Ltd., Osaka, Japan), while nothing was attached on the other side (Fig. 1). Ten microliter of the model compound (0.5 mM rhodamine B or 0.5 mM fluorescein sodium in PBS) was administered to each eye of the rat and rats were individually euthanized with pentobarbital sodium (100 mg/kg) intraperitoneally at each time point (10 min, 2 h, 8 h). After which, the (lower) eyelid skin was excised from rats by making an incision in the skin of the cranium, peeled away towards the eyelids. At the palpebra, skin was cut along the palpebral edge. The skin-free palpebra was then removed by cutting along the orbital arc (Maistrello et al., 1973). Thereafter, the excised rat lower eyelid skin was washed thrice with 1.0 mL PBS on each side of the dermis and epidermis and kept at -30°C until further processing (skin sectioning).

1.2.8 Measurement of Skin Impedance

Excised hairless rat abdominal skin or eyelid skin (either for full-thickness or stripped skin) was placed between Franz diffusion cells. PBS was added to the stratum corneum and dermis sides. Skin impedance was determined by an impedance meter (10 Hz AC, Asahi Technolab, Tokyo, Japan).

1.2.9 Histomorphological observation of under eyelid and abdominal skin

The skin samples, from hairless rat eyelid skin and abdominal skin, were cut vertically using a razor blade, embedded in supercryoembedding medium, and they were allowed to freeze using isopentane, and cooled with dry ice. Skin slices (10 μm thickness) were made using a cryostat (CM3050, LEICA, Wetzler, Hessen, Germany).

Hematoxylin and Eosin (H.E.) Staining. The obtained skin section was stained with hematoxylin and eosin. The prepared specimen was observed for its morphology with an optical microscope (DMWBI-223 Digital Biological Microscope, Shimadzu Corporation).

Nile Red Staining. The cryosectioned skin was treated with Nile red in acetone solution (500 mg/mL) with 4% potassium hydroxide solution (Sheu et al., 2003). After preparing the specimen, it was observed under a confocal laser scanning microscope (CLSM) (Fluoview FV1000 and software: FV10-ASW, Olympus, Tokyo, Japan) for the observation of neutral fat in the stratum corneum. The CLSM conditions were as follows: wavelength - 473 nm; scan speed - 200μ/pix; laser power - 1%; high voltage - 236V; gain - 1.125x; and offset - 0.

1.3.0. Statistical Analysis

All experimental data were tested for statistical significance ($p = 0.05$) using Student's *t*-test.

1.3 Results

1.3.1 In vitro skin permeation parameters

In vitro skin permeation experiment was conducted and the time course of the cumulative amount of these drugs permeated were determined in order to compare the permeation of six model compounds (antipyrine, diclofenac sodium, pilocarpine hydrochloride, aminopyrine, tranilast and lidocaine) having different lipophilicities (Log $K_{o/w}$)(Table 1) through eyelid and abdominal skin, Figure 2 shows the results. Typical lag time and following steady state permeation were found independent of drugs and skin sites. In addition, the drug permeation through eyelid skin was higher than that through abdominal skin independent of lipophilicity of the applied drugs. Table 3 summarizes permeation flux and permeability coefficient that were calculated from the skin permeation profiles. These permeation parameters were much higher for all model compounds administered via the eyelid skin compared to the abdominal skin. In addition, significant differences in the flux and permeability coefficient were observed for all model compounds when comparing the eyelid and abdominal skins. Furthermore, an eleven-fold higher tranilast permeation was observed in the eyelid skin than in the abdominal skin.

Table 1. Physicochemical properties of chemicals used in the study

Chemical	Molecular weight	Log $K_{o/w}$
Antipyrine	188.23	-1.51
Diclofenac sodium salt	318.13	-0.96
Fluorescein sodium salt	376.28	-0.61
Pilocarpine	208.26	0.17
Aminopyrine	231.29	1.07
Tranilast	327.33	1.80
Rhodamine B	479.02	2.28
Lidocaine	234.33	2.37

Table 3. Flux and permeability coefficient of model compounds

	Eyelid		Abdominal		
Chemical	Flux ($\mu g/cm^2/h$)	Permeability coefficient ($x10^{-7}cm/s$)	Flux ($\mu g/cm^2/h$)	Permeability coefficient ($x10^{-7}cm/s$)	Enhancement ratio($P_{eyelid}/P_{abdominal}$)
Antipyrine$^{\#,-}$	150 ± 13.9	8.36 ± 0.77	66.5 ± 7.23	3.69 ± 0.40	2.3
Diclofenac sodium salt $^{\#,-}$	72.2 ± 21.7	4.01 ± 1.20	12.0 ± 3.23	0.67 ± 0.18	6.0
Pilocarpine$^{\#,-}$	24.3 ± 4.95	49.1 ± 7.28	8.27 ± 1.63	18.8 ± 3.70	2.6
Aminopyrine$^{\#,-}$	745 ± 146	69.0 ± 13.6	335 ± 59.7	31.0 ± 5.53	2.2
Tranilast$^{\#,-}$	0.64 ± 0.23	3.66 ± 1.25	0.05 ± 0.02	0.34 ± 0.13	11
Lidocaine$^{\#,-}$	179 ± 14.0	151 ± 11.8	40.3 ± 10.6	34.2 ± 8.94	4.4

Significant difference ($P<0.05$) between eyelid and abdominal for flux$^{(\#)}$ and for permeability coefficient$^{(-)}$

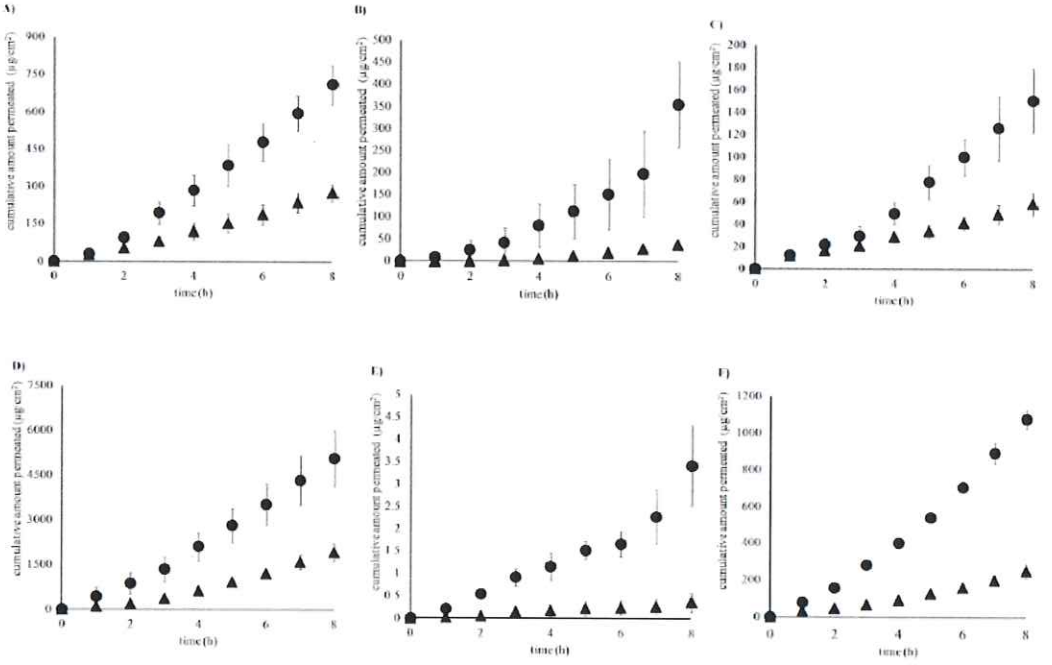

Figure 2. Time course of the cumulative amount of hydrophilic and lipophilic model drugs, A) antipyrine, B) diclofenac sodium, C) pilocarpine hydrochloride, D) aminopyrine, E) tranilast, F) lidocaine through eyelid (●) and abdominal (▲) skin. Each value represents a mean ±S.E. (n=3 – 5)

1.3.2 Drug concentration in skin

Among the model compounds, drug concentrations in skin were evaluated with tranilast and pilocarpine hydrochloride, which are important ophthalmic medications for patients with allergic disease and glaucoma, respectively. Figure 3 shows the result of drug concentrations in the whole skin and viable epidermis and dermis skin (VED) after topical application of these drugs on the eyelid and abdominal skins. Drug concentrations of tranilast and pilocarpine in the whole and viable epidermis/dermis skins in the eyelid skin were higher than those in the abdominal skin. Significant differences of pilocarpine were observed in the whole skin and VED between the eyelid and the abdominal skins, whereas for tranilast concentration, the VED shows a significant difference. About 3.7-fold higher pilocarpine concentration was observed in whole skin and VED, while about 1.4- and 2.8-fold higher tranilast concentrations were confirmed in the whole skin and VED, respectively.

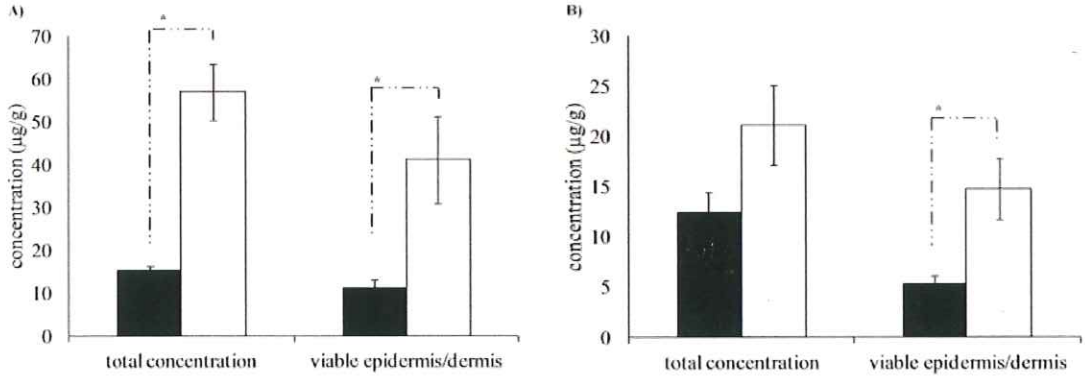

Figure 3. Skin concentration profile of pilocarpine (A) and tranilast (B) model compound in eyelid (□) and abdominal skin (■). Each value represents a mean ±S.E. (n=3). *$p<0.05$

1.3.3 Histomorphological evaluation of under eyelid and abdominal skin

With the interesting results showing high *in vitro* permeation profiles of hydrophilic and lipophilic drugs through the eyelid skin, further evaluation was conducted with impedance, morphology and neutral fat content/distribution of the eyelid and abdominal skins in hairless rats. Skin impedances of the intact eyelid and abdominal skins were much higher than those of stratum corneum-stripped skins. Intact abdominal skin has impedance values of 0.94 ± 0.20,

0.88 ± 0.19, 0.85 ± 0.16, 0.85 ± 0.15 for 0 min, 15 mins, 30 mins, and 1 h, respectively, from the start of the experiment. On the other hand, intact eyelid skin has impedance values of 0.49 ± 0.18, 0.47 ± 0.17, 0.45 ± 0.16, 0.39 ± 0.17 for 0 min, 15 mins, 30 mins, and 1 h, respectively. The values of skin impedance in the intact skins decreased at the beginning of the application period, and then the values became constant about 1 h thereafter. Furthermore, the abdominal skin has about two-fold higher impedance over 8 h compared to the eyelid skin.

Hematoxylin and eosin staining revealed that the stratum corneum in the abdominal skin was denser compared to the eyelid skin (Fig. 4). Moreover, Nile red staining images in the stratum corneum (the area of surrounded by a white line in Fig. 5) indicated that the neutral fat in the stratum corneum of the eyelid skin was evidently thinner and less compact compared to the abdominal skin.

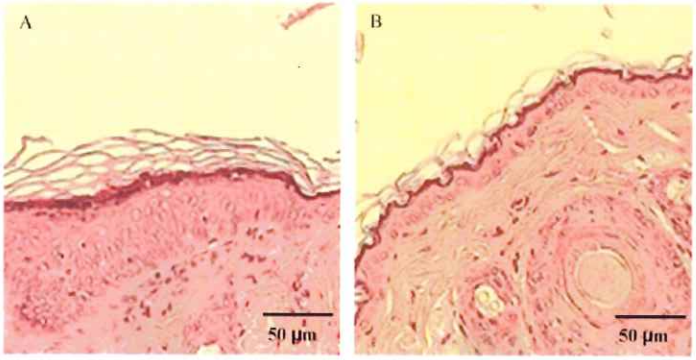

Figure 4. H.E. staining images of hairless rat skin. (A) abdominal skin; (B) eyelid skin. Magnification 400X

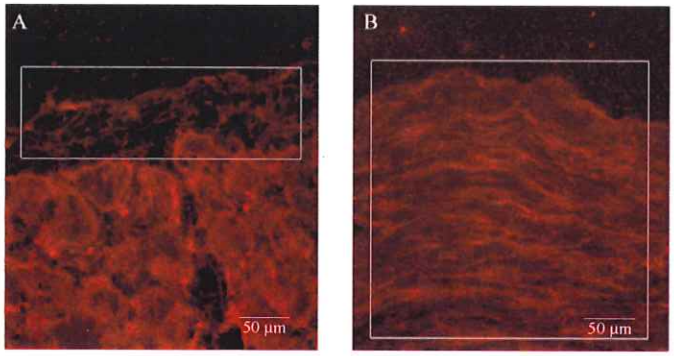

Figure 5. Nile red staining images of neutral lipids in stratum corneum of hairless rat skin enclosed in white box. (A) eyelid skin; (B) Abdominal skin. Magnification 800X

1.3.4 In vivo eyelid percutaneous absorption studies

With the concept of administering drugs to the conjunctiva through the eyelid skin, *in vivo* absorption studies were conducted with rhodamine B and fluorescein sodium salt as a lipophilic and a hydrophilic model dye compound, respectively. Figure 6 shows the drug distribution in skin after application of its solution by eye drops or through the (lower) eyelid skin. Presence of rhodamine B and fluorescein sodium administered as eye drops were markedly observed in the conjunctiva as indicated by the fluorescence in the images 10 min after administration, while absent in 2 and 8 h. For topical administration on the eyelid skin, a stronger intensity of the fluorescence given off by the model compounds was observed over time, which indicates greater amount of the dye compound in the conjunctiva.

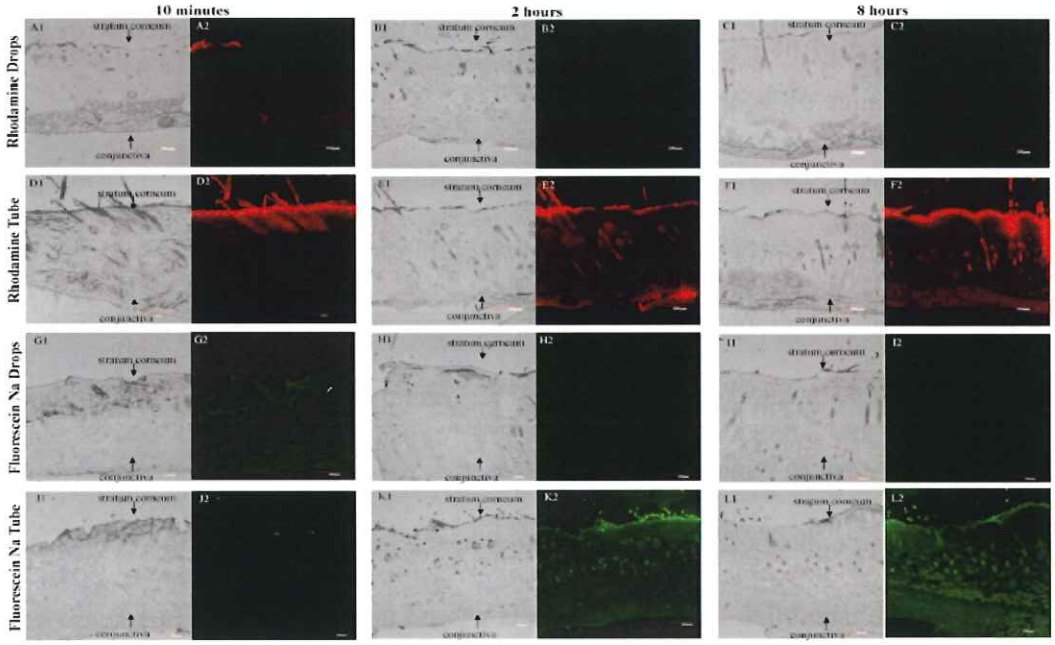

Figure 6. Photomicrographs of rat eyelid skin under CLSM after in vivo absorption studies. Transmission Images (A1 – L1); Confocal laser scanning images (A2 – L2)

1.4 Discussion

The delivery of ophthalmic medications remains a challenge up to this date. Bioavailability for eye drops is poor, amounting to at best 10% of the applied dose, since the eye is protected by a series of complex defense mechanisms that hinders the achievement of an effective drug

concentration within the target tissue of the eye. Frequent instillations of eye drops are often required to achieve the expected therapeutic benefit that is inconvenient and is often associated with adverse effects. (Li *et al.*, 2008; Gan *et al.*, 2010; Wang *et al.*, 2011; Kumar and Sinha, 2016; Akhter et al., 2016). On the other hand, transdermal drug delivery systems offers greater patient comfort while allowing a constant supply of drug at the application site and thus provides superior pharmacokinetic profile. A few studies reported the usefulness of the drug permeation through the eyelid skin (Kimura et al., 2007, Isowaki et al., 2003) and evaluated drug concentration in the conjunctiva after *in vivo* experiment. However, no reports have been published on the influence of drug lipophilicity on the (lower) eyelid skin permeation and its comparison between eyelid and abdominal skin permeation. Thus, in the present study, drug delivery within the ocular region through the eyelid skin was investigated with several drugs having a wide range of lipophilicity.

In order to demonstrate the proposed idea of administering medications through the eyelid skin, *in vitro* skin permeation and drug concentration in the eyelid VED were evaluated. Considering that sufficient human skin for a large number of skin permeation studies was usually unavailable because of ethical issue, hairless rat skin was used in this study. Moreover, hairless rats are easy to handle and manipulate (i.e., docile behavior), hence the most feasible animal to test the concept of delivering drugs to the conjunctiva via the eyelid skin. Several reports have published that hairless rat skin is a good alternative for human skin membrane to evaluate skin permeation profiles and permeability coefficient of drugs from aqueous solution (Watanabe et al., 2011; Morimoto et al., 1992; Abd et al., 2016; and Jung et al., 2014). Skin permeation profiles of several model drugs through the excised rat skin were measured to determine their flux and permeability coefficient in this study. Among various skin regions of the hairless rat, abdominal skin has often been used to evaluate skin permeation of drugs. Thus,

skin permeation of model compounds was compared with hairless rat eyelid and abdominal skin to elucidate feature in the skin permeation of drugs through (lower) eyelid skin.

Since topically applied drugs are mostly absorbed into the systemic circulation through the cutaneous vessels, prolonged retention of the drugs might be difficult below the application site. In normal (healthy) skin, 97-98% amount of drugs penetrated through the stratum corneum are taken into the microcirculation located beneath the basal layer of the epidermis (Kimura et al., 2007). However, the possibility of direct transport of drug to the conjunctiva after its topical skin application should be evaluated with *in vitro* permeation experiment, because skin permeation and concentration could be calculated with Fick's second law of diffusion model (Sugibayashi et al., 2010).

The ratio or fraction of topically applied drugs into the systemic circulation or the deeper cutaneous or subcutaneous tissue using an *in situ* experimental model in hairless rats were determined in our previous study (Sugibayashi et al., 1999; Hasegawa et al., 2007). Simply, most of the drug fraction penetrating the skin after topical application is taken up by the cutaneous blood flow, while some directly migrates into deeper tissues such as the subcutis and the muscle. In our previous study, topical application results to high drug concentration in subcutis and surrounding tissues. Thus, high drug concentration in the conjunctiva can be obtained by topical application through the eyelid skin.

Percutaneous absorption of drug molecules is of particular importance in the case of transdermal drug delivery systems, they should be able to cross the permeability barrier of the skin, the stratum corneum. Moreover, the lipids of the stratum corneum are important regulators against skin permeability of topically applied drugs (Feingold, 2009; Pappas, 2009). Morphological differences in the various anatomic sites of skin exist. Ya-Xian Z et al. (1999) reported that variations in the number of cell layers of the stratum corneum was observed according to the anatomical location of human skin. The number of stratum corneum layers in

the eyelid was 8 ± 2 (n=16, mean ± SD) and abdomen 14 ± 4 (n=44, mean ± SD) and a significantly higher Transepidermal Water Loss (TEWL) value was observed in the eyelid compared to abdominal skin. In addition, Pratchyapruit et al. (2007) reported that eyelid showed high TEWL value like other facial skin. The skin surface hydration was as high as that of adjacent skin regions even though the eyelid skin has extremely low amounts of surface lipid unlike its neighboring skin regions. The present results obtained from skin impedance and H.E. staining also corresponded to these reports. Moreover, based on our experimental result, the stratum corneum of eyelid skin had a lesser neutral fat content. These supports our findings in which a significant difference was observed between the permeability coefficient of the model compounds through the eyelid skin as compared to the abdominal skin. In terms of the relationship between molecular weight and log*P*, a strong positive relationship exists. Many reports have been published on the relationship of *MW* and log *K*o/w on the skin permeation through abdominal skin (Morimoto et al., 1992; Potts and Guy, 1992; Chen et al., 2013). Although there is a regional difference in the skin permeation of drugs, skin permeation of drugs through eyelid skin would be expressed with a function of MW and log Ko/w. In the present experiment, only several drugs were used to compare the skin permeation differences between abdominal and lower eyelid skins. Thus, it was difficult to explain the effect of these parameters on the skin permeation of drugs through eyelid skin.

To further confirm drug delivery via the eyelid skin into the conjunctiva, *in vivo* experiment was performed with fluorescent markers of rhodamine B and fluorescein sodium salt. The disposition of these model compounds in the conjunctiva increased with the passage of time. The intensity of the fluorescence 8 h after administration via the eyelid skin was markedly higher than that of eye drop administration. There was no fluorescence observed at 2 h following eye drop administration, indicating the absence or very low distribution of the model compounds in the conjunctiva. The present results correspond to a study utilizing conventional

eye drops which resulted to lower bioavailability (Lux et al., 2003). Rapid and extensive loss caused by drainage and high tear fluid turnover of the instilled eye drops may be the main reason for the disappearance of the fluorescence 2 h after administration. Moreover, contact time of the model compound with ocular tissues is relatively short because of the constant production of lacrimal fluid. In contrast, transdermal drug delivery through eyelid offers a steady concentration of the model compound for an extended period of time. This further supports the findings of our *in vivo* absorption studies wherein fluorescence were evident even after 8 h while being unnoticeable for eye drops. We have confirmed the migration of the model drugs from the eyelid skin into the conjunctiva and eyeball. Although drug concentration and its distribution profile into the eyeball is not reported in this study, a preliminary study revealed that administration of model compounds via the eyelid skin were detected in eyeball homogenates, suggesting the possibility of drug delivery into the conjunctiva and eyeball. The mechanism of drug migration from eyelid skin to eyeball was not revealed yet in the present study. Currently, we assume that drug partitioning from eyelid skin to lacrimal fluid was the primal route for drug migration into eyeball.

There is a need to address the bioavailability and the delivery of drugs applied on the eyelid skin and as eye drops. The bioavailability resulting from eye drop administration is presumed to be very low. In this study, the permeability coefficient of drugs applied on eyelid skin was much higher than that of abdominal skin. The obtained permeability coefficients from the lowest ($3.66 \pm 1.25 \times 10^{-7}$ cm/s for tranilast) to the highest ($151 \pm 11.8 \times 10^{-7}$ cm/s for lidocaine)(Table 3) are comparable or higher than those drugs which are already marketed as transdermal delivery systems. The targeting ability of eye drops to the conjunctiva is high due to its direct contact with the conjunctiva. However, its elimination is high and at the same time, drug concentration in the conjunctiva may not be sustained (see Fig. 6). Despite lacking direct

contact with the conjunctiva, eyelid administration as a delivery method exhibits the advantage of having a controlled drug delivery as shown in Fig. 6.

Since the eyelid skin is known to be thinner than the conventional skin administration sites, it offers higher drug permeation as evidenced by the results of this study. Developing formulations dedicated to eyelid administration such as eyelid patch is recommended. In fact, ointments are often used for night time application but it is associated with discomfort due to greasiness, tear film instability, and uncertain drug disposition following eye shutting while asleep (Desai and Lee, 2007). Thus, eyelid skin application is seen to be beneficial even during sleep when the use of liquid and semi-solid eye preparations deemed impossible.

1.5 Conclusion

The drug concentration in rat conjunctiva following application on the eyelid skin was higher than that of the conventional eye drops. In addition, drug permeation through eyelid skin was higher than that of the abdominal skin regardless of lipophilicity. Diclofenac sodium salt and tranilast significantly showed about 6-folds and 11-folds higher permeation coefficients, respectively, than the abdominal skin. With these preliminary findings, the eyelid skin is a promising site for the administration of ophthalmic drugs. Further *in vivo* studies will be conducted to establish the distribution of drugs in the various parts of the ocular regions following eyelid administration.

Chapter 2

Iontophoresis-aided drug delivery into the eyeball via eyelid skin

2.1 Introduction

Eye drop application remains the most common method for treating eye diseases, such as glaucoma and conjunctivitis, because of its simple application method and rapid delivery of drugs to ocular target sites. However, the complex anatomy and physiology of the ocular tissues impede the bioavailability and controlled delivery of drugs administered as eye drops [1-5]. The use of eye ointment and gelled ophthalmic solution may reduce drug retention because discomfort and irritation in the eye will ensue [6,7]. Recently, lower eyelid skin has gained attention as a drug delivery site for the eye [8,9]. Because the conjunctiva is located proximately to the eyelid skin, application of a drug onto the lower eyelid skin can be done even while the patient is asleep and during which drug retention at the application site can be expected. In addition, the administered drug can easily be discontinued at the application site. Moreover, because the eyelid skin has a thinner stratum corneum and lower amount of neutral fat compared with the abdominal skin, it offers an advantage of higher drug permeability [10].

In our previous study, we established that drugs applied to the lower eyelid skin could migrate to the conjunctiva, and the drug concentration was maintained in the conjunctival sac for a long duration compared with eye drop application. However, the migration of drugs to the eyeball after eyelid skin application was considered to be lower than eye drops because drugs, in the case of eye drops, were delivered directly onto the eyeball [3]. In this case, we considered the necessity of utilizing physical approaches, such as iontophoresis (IP), to further promote percutaneous absorption and delivery to the eyeball via the lower eyelid skin.

IP is a non-invasive technique to increase the penetration of ionized compounds into the body across the epithelial surface, including the skin and ocular surface. The basic principle of IP is that ions with opposing charges attract and ions with the same charge repel. Moreover,

ionized substances are driven into the tissue by electrorepulsion and electroosmosis. This method has the potential to control the penetration of drugs depending upon the applied current density and application time. Because of its recognizable advantages, such as the ease of application, non-invasiveness, and increased drug penetration directly into the target tissue, IP has been used to deliver drugs across various barriers such as the skin and eyes [11,12]. Moreover, topical preparations utilizing IP have already been put to practical use in ocular drug delivery by direct application of an IP device to the cornea or the eyelids but none have been done on the lower eyelid skin.

With a limited number of studies investigating the delivery of drugs into the eyeball through eyelid skin with IP, we were prompted to investigate the effect of IP application on drug permeability through the eyelid skin. In the present study, pilocarpine, a muscarinic agonist for glaucoma, was used as a model drug. Moreover, two fluorescent dyes (fluorescein sodium and rhodamine B) were used to determine the *in vivo* distribution of drugs in the eyeball after topical application onto the lower eyelids and eye drops application.

2.2 Materials and methods

2.2.1 Materials and experimental animals

Pilocarpine hydrochloride was purchased from Sigma-Aldrich (St. Louis, MO, USA). Fluorescein sodium and rhodamine B were purchased from Wako Pure Chemical Industries, Ltd. (Osaka, Japan).

Male hairless rats (WBM/ILA-Ht, 8 weeks of age, body weight of 220–260 g) were obtained from the Life Science Research Center, Josai University (Sakado, Saitama, Japan) or Ishikawa Experimental Animal Laboratories (Fukaya, Saitama, Japan). All animal handling and experiments were in accordance with the ARVO statement for the use of animals in

ophthalmic and vision research as well as approved by the Institutional Animal Care and Use Committee of Josai University with the approval number H29003.

2.2.2. Preparation of donor solution and skin membranes

Pilocarpine aqueous solution was prepared by dissolving it in phosphate-buffered saline (PBS; pH 7.4) to reach a concentration of 10 mg/mL. Fluorescein sodium (1 mM) or rhodamine B (1 mM) was prepared by dissolving it in PBS pH 7.4.

Whole abdominal and (lower) eyelid skin were freshly excised from hairless rats previously shaved under three types of anesthesia (0.375 mg/kg medetomidine, 2.5 mg/kg butorphanol, 2 mg/kg midazolam) administered intraperitoneally. The excised skin was cleaned with PBS pH 7.4.

2.2.3. Preparation of an Ag/AgCl electrode for IP

Silver wire with a diameter of 1.0 mm was cut to a size of 4 cm. It was attached to a copper plate, then immersed in a plastic container filled with 3% NaCl solution with VC Stabilizer (SJ-1061, ATTO Co., Tokyo, Japan). The Ag/AgCl electrode was fabricated by applying a current of 5 min. The silver wire previously cut to 4 cm was used as the Ag electrode.

2.2.4 In vitro skin permeation experiment[3]

Skin permeation experiments were carried out using a Franz type vertical diffusion cell. Excess subcutaneous fat was trimmed off from the excised intact abdominal skin, but no trimming was done for the eyelid skin. The eyelid skin was placed on a stabilizing apparatus with an effective diffusion area of 0.0707 cm^2 before it was set in a vertical diffusion cell. The abdominal skin sample was directly set in a vertical type diffusion cell with an effective diffusion area of 1.77 cm^2. One mL of PBS, which corresponded to the donor solution, and contained no permeant was applied to the epidermis side, and 6.0 mL of PBS was applied to

dermis side of the skin to reach an equilibration state for approximately 1.0 h. After an hour, the PBS on the epidermis side was replaced with the same volume of donor solution (1% aqueous pilocarpine) to commence the permeation experiment. Moreover, during IP application, the Ag and AgCl electrodes were placed in the donor and receiver solution, respectively. The IP device (ADIS-HP v.6, ADTK 98, MTH 30, Hisamitsu Pharmaceutical Co. Inc.) with the current set at 0.3 mA/cm^2, was applied for 8 h. The receiver solution was stirred with a stirrer bar on a magnetic stirrer and maintained at 32°C using a thermostatically controlled heater throughout the experiments. An aliquot (500 µL) was withdrawn from the receiver chamber and the same volume of fresh PBS was added to the chamber to keep the volume constant. The penetrant concentration in the receiver chamber was determined by high-performance liquid chromatography (HPLC).

2.2.5. In vivo skin permeation studies

Rats were anesthetized with three types of anesthesia as described above. A Teflon tube with an effective permeation area of 0.13 cm^2 was glued onto the lower eyelid skin using cyanoacrylate bond (Aron Alpha® Konishi Co. Ltd., Osaka, Japan) (Fig. 1). Prior to IP application, two Teflon tubes were attached side by side on the lower eyelid skin, and 60 µL of pilocarpine aqueous solution was loaded into one tube and PBS was loaded into the other. The Ag electrode was placed in the tube containing pilocarpine aqueous solution, and the AgCl electrode was placed in the tube containing PBS. The applied current was 0.3 mA/cm^2. IP load was applied for 0.5 or 2 h. Throughout the experiment, the animal body's temperature was maintained at 37°C using a thermo-regulated carpet. After the application period, the rat was euthanized with *i.p.* injection of pentobarbital sodium (100 mg/kg). Lower eyelid skin and the eyeball were excised from the rats using the method of Maistrello et al., 1973 [13]. The collected samples were reduced in size using scissors, and 0.5 mL of acetonitrile was added

prior to homogenization at 12,000 rpm and 4°C for 5 min using a homogenizer (Polytron PT 1200 E, Kinematica AG, Littaue-Lucerne, Switzerland). The sample homogenate was mixed and then centrifuged at 15,000 rpm and 4°C for 5 min. The compound concentration in the resulting supernatant was determined by liquid chromatography–tandem mass spectrometry (LC-MS/MS).

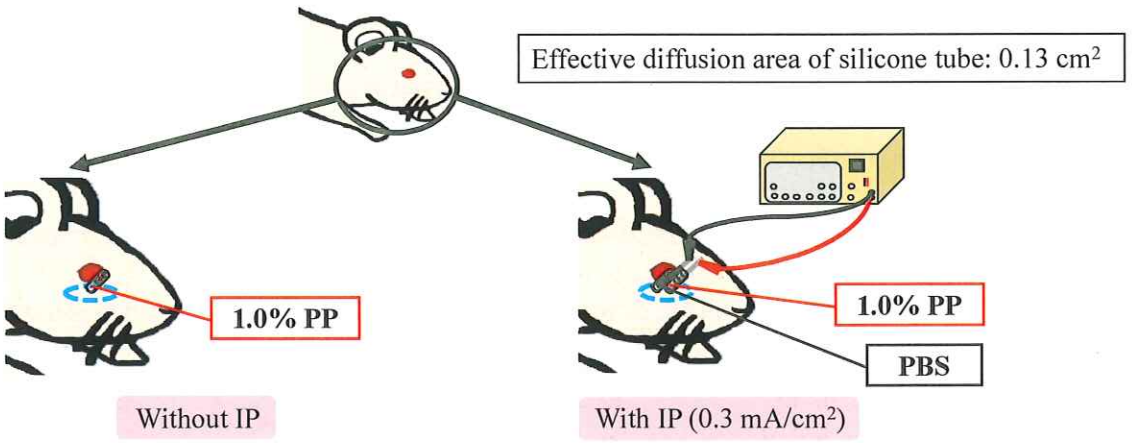

Figure 1. Illustration for in vivo permeation study using IP

2.2.6. In vivo distribution study

Six rats were used in this part of the study. Fluorescent dyes (rhodamine B and fluorescein sodium) were used as the model drugs to examine their distribution. Three rats were designated for transdermal eyelid delivery with IP, and the other three were designated for eye drop administration. Prior to IP application, two Teflon tubes were attached side by side on the lower eyelid skin and 60 μL of (fluorescent dyes) was loaded into one tube, and PBS was loaded into the other. For rhodamine B, the Ag electrode was placed in the tube containing rhodamine B and the AgCl electrode was placed in the tube containing PBS. Conversely, the Ag electrode was place in the tube containing PBS and the AgCl electrode was placed in the tube containing fluorescein sodium. The applied current was 0.04 mA/cm^2. IP load was applied for 8 h. Furthermore, 10 μL of the model drugs was administered as eye drops. Rats were individually

euthanized at each time point (0.5, 2, and 8 h). Eyeballs were excised using the method of Maistrello et al., 1973. The collected eyeball was washed five times with 1.0 mL PBS and kept at -30°C until further processing (see histomorphological observation).

2.2.7. Instrumental analysis of samples

HPLC: The obtained supernatant (20 μL) was injected into an HPLC system. The HPLC system (Shimadzu Co., Kyoto, Japan) consisted of a system controller (SCL-10A), pump (LC-20AD), degasser (DGU-20A$_3$), auto-injector (SIL-20A), column oven (CTO-20A), UV detector (SPD-20A), and analysis software (LC Solution). The column used was an Inertsil® ODS-3 4.6 mm × 150 mm, 5 μm (GL Sciences Inc., Tokyo, Japan). The column was maintained at 40°C, and the flow rate of the mobile phase (acetonitrile: 0.1% phosphoric acid = 5:95) was adjusted to 1.0 mL/min. Calibration was carried out with six different concentrations within a range of 0.1 – 100 μg/mL with a correlation coefficient of 0.9999.

LC-MS/MS: The obtained supernatant from the homogenates (10 μL) was injected into an LC-MS/MS system. The LC-MS/MS system consisted of a system controller (CBM-20A; Shimadzu), pump (LC-20AD; Shimadzu), auto-sampler (SIL-20ACHT; Shimadzu), column oven (CTO-20A; Shimadzu), detector (4000QTRAP; AB Sciex; Tokyo, Japan), and analysis software (Analyst® version 1.4.2; Shimadzu). The column was a Shodex ODP2HPG-2A 2.0 mm × 10 mm (Showadenko Inc; Tokyo, Japan), which was kept at 40°C. The mobile phase was acetonitrile:0.2% trifluoroacetic acid containing 40 mM ammonium acetate = 85:15, and the flow rate was 0.2 mL/min. Mass spectrometric quantification was carried out in the multiple reaction monitoring (MRM) mode, monitoring transition ions of *m/z* 209.1 to *m/z* 95.1 with collision energy of 36 eV in positive ion mode. Calibration was carried out with six different concentration within a range of 1– 1000 ng/mL with a correlation coefficient of 0.9999.

2.2.8. Histomorphological observation of eyeballs

The collected eyeballs from hairless rats were embedded in Tissue Tek® OCT compound (Miles Inc. Elkhart, N.J., U.S.), and were allowed to freeze using isopentane, and cooled with dry ice. Eyeball slices (10 μm) were made using a cryostat (CM3050, LEICA, Wetzler, Hessen, Germany). The obtained eyeball slices were viewed under a fluorescence microscope (BZ-X700, Keyence, Illinois, USA) at excitation and emission wavelengths of 495 and 515 nm, respectively, for fluorescein sodium, and 540 nm and 625 nm, respectively, for rhodamine B. Consistent conditions throughout the measurement were utilized to observe the distribution of each drug in the eyeball.

2.2.9 Statistical analysis

All experimental data were tested for statistical significance ($p < 0.05$) using Student's *t*-test.

2.3. Results

2.3.1. In vitro skin permeation

Figure 2 shows the time course of the cumulative amount of pilocarpine that permeated through the abdominal skin or lower eyelid skin. Table 1 summarizes the flux and permeability coefficient. The cumulative amount of pilocarpine that permeated showed a significant difference between the presence and absence of IP application, which was approximately 18-fold higher for abdominal skin and 7-fold higher for eyelid skin when IP was applied, indicating a significant permeation enhancement by IP application. In a comparison between pilocarpine permeation through lower eyelid skin and abdominal skin with IP application, drug permeation through eyelid skin was about 1.4 times higher than through abdominal skin. The dramatically lower permeation observed with abdominal skin was due to its thicker stratum corneum, which

acts as a barrier against drug permeation in the absence of IP application. On the other hand, the eyelid skin allowed higher drug permeation even in the absence of IP application because it has a thinner stratum corneum.

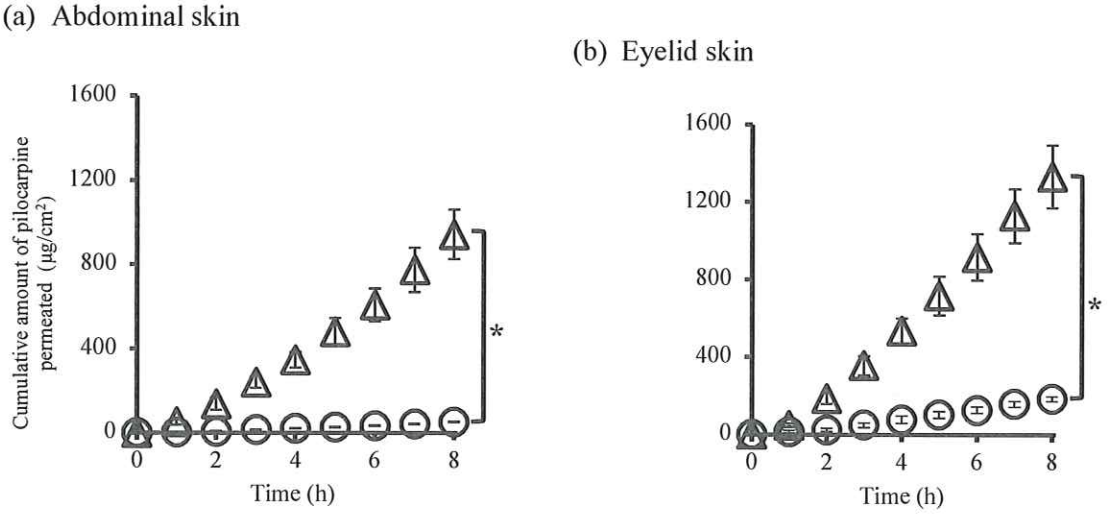

Figure 2. Effect of IP application on the cumulative amount of pilocarpine that permeated through abdominal skin (a) or eyelid skin (b). Symbols: △, with IP (0.3 mA/cm^2); ○, without IP. Each point shows the mean ± S.E. (n = 4 – 5). (*$p < 0.05$)

Table 1. Flux and permeability coefficient of pilocarpine

	Eyelid		Abdominal	
	Flux (μg/cm^2/h)	Permeability coefficient (× 10 $^{-7}$ cm/s)	Flux (μg/cm^2/h)	Permeability coefficient (× 10 $^{-7}$ cm/s)
Without IP	27.43 ± 3.30	6.33 ± 0.36	8.33 ± 0.40	2.18 ± 0.60
With IP	235.38 ± 18.20	62.5 ± 4.90	150.35 ± 15.80	38.15 ± 9.90
Enhancement ratio ($Flux_{\text{with IP}}/Flux_{\text{without IP}}$)		8.58		18.05

2.3.2 In vivo skin permeation

Figure 3 shows the pilocarpine concentration in eyelid skin and in the eyeball at 0.5 and 2 h after starting the permeation experiment. Different skin concentrations in the lower eyelid were observed after 0.5 h of IP application, but no difference in skin concentration due to IP application was observed after 2 h. In addition, significant differences were observed in the eyeball concentrations between the presence and absence of IP at 0.5 h. Furthermore, because no difference was found in the ocular concentration due to IP load over 0.5 and 2 h, it was

considered that the drug concentration in the eyes reached a steady state at 0.5 h after application. It was suggested from these data that the application of IP for a short period is effective for drug delivery to the eyeballs.

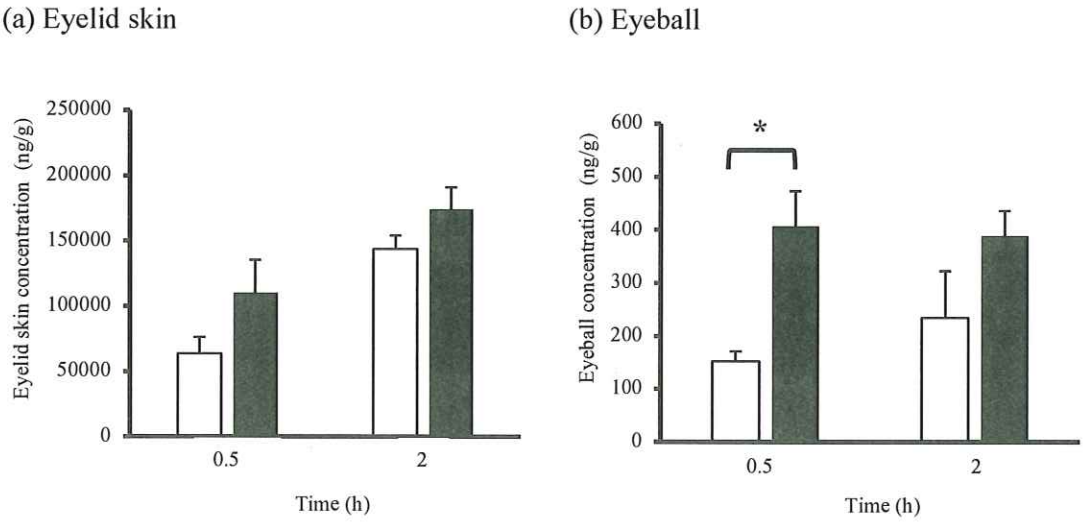

Figure 3. Effect of 0.5 or 2 h of IP application on the concentration of pilocarpine in eyelid skin (a) and eyeball (b). Symbols: □, without IP; ■, without IP (0.3 mA/cm^2). Each point shows the mean ± S.E. (n = 3). (*$p < 0.05$)

2.3.3. In vivo distribution studies

Fig.4 shows the drug distribution of rhodamine B and fluorescein sodium, lipophilic and hydrophilic model compounds, respectively, after application of each solution as eye drops or topical application onto the lower eyelid skin with IP. The presence of rhodamine B or fluorescein sodium was distinctly seen in the eyeball at 0.5 h after eye drop administration, but the intensity of fluorescence diminished at 8 h post eye drop administration. For topical administration into the eyelid skin with IP, a stronger fluorescence intensity from the model compounds was observed over time independent of their lipophilicities, indicating greater amount of each compound in the eyeball. In addition, localization of the dye in the posterior chamber of the eyeball at 8 h was clearly observed.

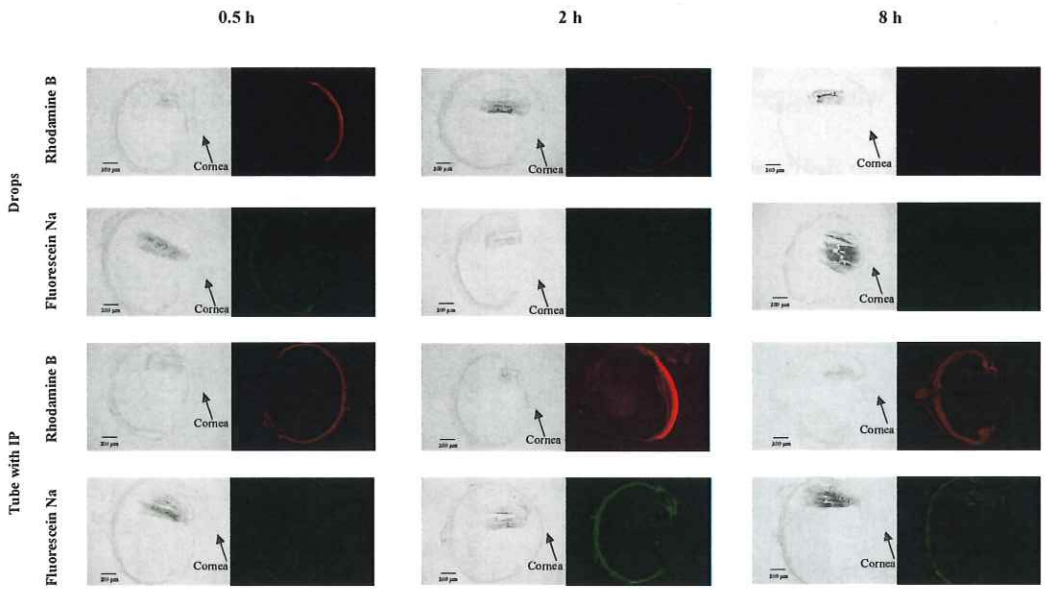

Figure 4. Photomicrographs of rat eyeballs after *in vivo* distribution studies. All observations were performed without changing observation conditions for each drug.

2.4. Discussion

In all ocular therapies involving medicines, the route of drug delivery plays an important role. Conventional ocular dosage forms, such as eye drops, remain a common method of drug delivery. Eye drops are well accepted by patients and have rapid and localized drug action. Nevertheless, eye drop delivery is associated with low ocular bioavailability, toxicity, poor patient compliance, and systemic side effects [14]. Therefore, an alternative method of delivering drugs, through the lower eyelid skin, was evaluated in the present study.

Hairless rats were used as a model animal, because it was the most feasible animal compared with larger animal models to test our concept of drug delivery. Moreover, several reports documented that hairless rat skin is a good alternative for human skin membrane to evaluate the skin permeation of aqueous drugs [3;15-16].

In the present study, we investigated the effect of a physical penetration-enhancement method, IP, in the delivery of pilocarpine and two fluorescent dyes into the eyeball. Pilocarpine hydrochloride was selected as a positively charged model drug that has a preferable nature for

iontophoresis. Understanding drug migration into the eyeball from the eyelid skin confirms the feasibility of iontophoresis-aided drug delivery. Ocular iontophoresis is employed as a non-invasive and safe physical method to drive drugs into the anterior and posterior segments of the eye, penetrating ocular tissues with poor permeability such as the corneal epidermis. It can improve the efficiency and security of ocular drug delivery [17]. Ocular IP devices set electrodes under the eyelid or on top of cornea in a drug solution-filled cap to provide electrical field. Our study demonstrated that the delivery of drugs via the eyelid skin with the aid of IP facilitated the migration of drugs into the eyeball. Pilocarpine is a cholinergic agonist used for the treatment of glaucoma and ocular hypertension. Its action is intended to be localized in the eyeball. Hence, optimum concentrations of pilocarpine have to reach the eyeball to exert its therapeutic effect.

Pilocarpine, a hydrophilic molecule with a positive polarity, may not be readily delivered into the skin because the skin has relatively high impedance, which is mainly associated with a high barrier function of the stratum corneum. During IP application, skin resistance decreased and ion concentration increased in the stratum corneum. Positively charged pilocarpine was repelled into the skin by an identical charge on the electrode surface placed over it, allowing the delivery of the substance during electric current stimulation. At the end of the current flow, the ion concentration in the skin returned to physiological levels [18]. Furthermore, the electrical potential gradient introduced a second driving force for molecular transport in addition to the concentration gradient across the skin membrane. This mechanism is attributable to a higher permeation rate of pilocarpine, as observed in Fig. 2, with IP application.

In vivo study reveals that the concentration of pilocarpine in the eyeball is significantly increased by 3-fold with IP application over 0.5 h. For the 2-h application, however, it did not significantly increase with IP, suggesting that the steady state of pilocarpine had been reached

within 0.5 h after IP application. The appropriateness of a 2-h period observation for the *in vivo* study was supported by the finding of Birmingham et al. 1979, in which pilocarpine had a maximal effect at 2 h [19].

In the management of glaucoma, pilocarpine induces contraction of smooth muscle cells in the ciliary body, which leads to an increase in the aqueous humor outflow by widening the trabecular meshwork and Schlemm's canal. This leads to a decrease in the intraocular pressure [20]. In our study, pilocarpine possibly migrated into the eyeball via the non-corneal (conjunctival–scleral) pathways. This pathway favors the passage of hydrophilic drugs (i.e., pilocarpine) permitting direct access to the intraocular tissues of the posterior segment of the eyes. Moreover, trans-scleral iontophoresis has been shown to significantly increase the vitreous levels of drug, confirming the high concentration of pilocarpine in the eyeballs [21,22]. Of note, about 400 ng/g pilocarpine was detected in the eyeball following topical administration through the eyelid skin. The concentration was within the therapeutic range for the reduction of intraocular pressure in open-angle glaucoma [23].

In vivo distribution studies of two fluorescent dyes further supported the findings of our *in vivo* skin permeation studies. Topical administration with IP showed that corneal permeation of the both fluorescein sodium and rhodamine B was observable 0.5 h after administration (Fig. 4). Our findings were in agreement with previous study where the concentrations of dyes were observed in the anterior part of the eyeball 0.5 h after administration [24,25]. Furthermore, the concentration of dyes peaked 2 h post administration with IP, especially with fluorescein sodium, a hydrophilic dye. Pilocarpine, being a hydrophilic molecule, may also exhibit a similar pattern of distribution into the eyeball.

Histomorphological analysis revealed the migration of dyes from the eyelid skin into the anterior chamber of the eyeball possibly through the conjunctiva and sclera, because these tissues have rich networks of capillaries. This was supported by the findings of Chien et al.,

1990 and Nasir et al., 2017, wherein topically applied drugs reach the ciliary body and retina through the conjunctiva and sclera [25,26]. At 8 h, the dyes reached the posterior chamber of the eyeball, indicating that there was a constant delivery of the drugs into the eyeball after topical administration onto the lower eyelid skin with IP in contrast to eye drops application (Fig. 4).

The eyelid skin is known to be thinner than conventional skin, and it offers higher drug permeation into target tissues. With an aid of physical permeation enhancement methods, it is expected that permeation rates will exceed normal drug delivery methods. IP application on the eyelid skin allowed the delivery of pilocarpine to the eyeballs. The concentration of pilocarpine after eye drop is important and the measurement of its pharmacokinetic profile as well as the disposition in the eye will be considered in succeeding studies. Drug disposition was investigated in this paper using fluorescent dyes, fluorescein sodium (hydrophilic) and rhodamine-B (lipophilic), which were applied using eye drops and topical application on eyelid skin with IP. This drug delivery method should be tested with other ocular drugs as an alternative to eye drops.

2.5 Conclusion

The use of IP enhanced the penetration and delivery of drugs into the eyeball after topical application onto the lower eyelid skin. Higher concentrations of pilocarpine were detected in the eyeball after IP application. Histomorphological evidence confirmed the migration of dyes into the posterior chamber of the eyeball after topical administration onto the lower eyelid skin with IP. Prolonged drug application on eyelid skin may be undesirable when compared to conventional arm or chest patches applied at daytime. However, during sleep, drug administration through eyelid skin is thought to be a favorable method of drug delivery into the eyeball.

Chapter 3

Pharmacokinetic and tissue distribution studies of pilocarpine and tranilast following eyelid skin delivery

3.1 Introduction

Glaucoma and other ocular diseases such as conjunctivitis and eye infections, require instantaneous management and entail frequent eye drop instillation particularly in chronic conditions. While instillation of eye drops is viewed as a simple task, studies have shown that patients often have difficulty instilling eye drops, a challenge which leads to poor adherence (Sayner et al., 2016; Schwartz et al., 2013; Lavik et al., 2011). Instilled drugs show low bioavailability since they are rapidly eliminated from the lacrimal fluid by drainage of extra solution, induced lacrimation, and tear turnover. Moreover, the frequent administration of eye drops lead to significant systemic absorption which may result in undesirable side effects (Ustundag-Okur et. al., 2014; Ramsay et al., 2018).

Eyelid skin, the thinnest skin layer, has shown to be more permeable to some drugs than the skin localized in different areas in the body (See et al., 2017). The number of cell layers in the stratum corneum of human eyelid skin is 8 ± 2 while it is 14 ± 4 in the abdominal skin (Ya-Xian et al., 1999). Generally, the thinner the stratum corneum, the greater the skin permeation. Topical application of drugs onto the lower eyelid skin is noninvasive and it has sustained delivery features maintaining a constant drug concentration beneath the application site for a longer duration (See et al., 2018; Kimura and Tojo, 2007; Isowaki et al., 2003).

It is very important to explore the possibility of extending and prolonging the delivery of drugs into the eyes as the eyelid is proximately located to the conjunctiva, which serves as a reservoir for drugs. In this case, drugs may not be eliminated rapidly as it is localized in this vasculature allowing a sustained delivery of the drugs into the eyeball from the eyelid skin. Of note, the conjunctiva has a direct contact with the anterior and posterior regions of the eyeball,

the target area in most ocular diseases. Also, it is 2 to 30 times more permeable to drugs than the cornea (Davies, 2000).

There has been no investigation that such topical application onto lower eyelid skin may be useful for the treatment of chronic eye diseases. However, the only evidence that exists is our previous work wherein the eyelid skin was found to be more permeable to drugs than the abdominal skin regardless of their lipophilicities. To further elucidate the critical value of delivering drugs onto the eyeball through the eyelid skin, pharmacokinetic studies of pilocarpine and tranilast were conducted. Our pharmacokinetic results appeared to confirm the hypothesis and additionally, these results were verified by direct pharmacodynamic study of pilocarpine in rats.

3.2 Materials and methods

3.2.1. Materials and experimental animals

Pilocarpine hydrochloride was purchased from Sigma-Aldrich (St. Louis, MO, USA). Tranilast was purchased from Tokyo Chemical Industry Co. Ltd. (Tokyo, Japan).

Male hairless rats (WBM/ILA-Ht, 8 weeks of age, body weight of 220 – 260 g) were obtained from the Life Science Research Center, Josai University (Sakado, Saitama, Japan) or Ishikawa Experimental Animal Laboratories (Fukaya, Saitama, Japan). All animal handling and experiments were in accordance with the ARVO statement for use of animals in ophthalmic and vision research as well as approved by the Institutional Animal Care and Use Committee of Josai University with the approval number JU 18003.

3.2.2. Preparation of solutions for administration

Pilocarpine hydrochloride (1%) solution were prepared by dissolving the drug in sufficient amount of phosphate buffered saline pH 7.4 to reach the desired concentration.

Tranilast (0.1%) solution were also prepared using the same solvent as pilocarpine to reach the desired concentration.

3.2.3. Tissue distribution studies

Rats were anesthetized with three types of anesthesia (0.375 mg/kg medetomidine, 2.5 mg/kg butorphanol, 2 mg/kg midazolam) administered intraperitoneally. A Teflon tube (internal diameter of 0.48 cm and height of 2 cm) was glued onto both lower eyelid skin using cyanoacrylate bond (Aron Alpha Konishi Co. Ltd., Osaka, Japan). A hundred microliters of the compounds were instilled into the attached tube on both eyes of the rats. At a predefined time point (0.25, 2, 4, 6, 8 h) after drug administration, the rat was euthanized with pentobarbital sodium (100 mg/kg) intraperitoneally. Blood samples of 200 μL were collected at pre-defined time points and immediately placed in heparin-coated plastic tubes prior to euthanasia. The samples were centrifuged for separation of plasma and the supernatant plasma was transferred into a separate tube and analyzed. After the application of euthanasia, the lower eyelid skin, conjunctiva, and eyeball were collected and weighed. The collected samples were reduced in size using scissors, and 0.5 mL of acetonitrile was added prior to homogenization at 12,000 rpm and 4°C for 5 min using a homogenizer (Polytron PT 1200 E, Kinematica AG, Littaue-Lucerne, Switzerland). The sample homogenate was mixed and then centrifuged at 15,000 rpm and 4°C for 5 min. The compound concentration in the resulting supernatant was determined by LC-MS-MS.

3.2.4. LC-MS-MS

The withdrawn sample containing the compound (200 μL) was mixed with 200 μL acetonitrile and centrifuged at 4°C for 5 min. The obtained supernatant (10 μL) was injected into a LC/MS/MS system. The LC/MS/MS systems consisted of a system controller (CBM-

20A; Shimadzu), pump (LC-20AD; Shimadzu), auto-sampler (SIL-20ACHT; Shimadzu), column oven (CTO-20A; Shimadzu), detector (4000QTRAP; AB Sciex; Tokyo, Japan), and analysis software (Analyst® version 1.4.2; Shimadzu). The column was Shodex ODP2HPG-2A 2.0 mm x 10 mm (Showadenko Inc; Tokyo, Japan), which was kept at 40°C. For pilocarpine, the mobile phase was acetonitrile:0.2% trifluoroacetic acid containing 40 mM ammonium acetate = 85:15, and the flow rate was 0.2 mL/min. Mass spectrometric quantification was carried out in the multiple reaction monitoring (MRM) mode, monitoring transition ions of *m/z* 209.1 to *m/z* 95.1 with collision energy of 36 eV in positive ion mode. For tranilast, the mobile phase was acetonitrile:0.05% formic acid containing 5 mM ammonium acetate = 80:20, and the flow rate was 0.2 mL/min. Mass spectrometric quantification was carried out in the multiple reaction monitoring (MRM) mode, monitoring transition ions of *m/z* 328.0 to *m/z* 191.2 with collision energy of 36 eV in positive ion mode.

3.2.5. Pupil Size Determination

Anesthetized rats (n=6) were divided into two groups. The first group was administered with 10 μL of pilocarpine solution by eye drops while the other group was administered with the same solution in the form of a tube glued directly on the lower eyelid skin of hairless rats. The change in pupil size was determined using a digital microscope (VHX-5000). The area of the pupil was calculated using a program VH-M100 XY Measurement system (VHX-5000, Keyence co. LTD, Osaka, Japan).

3.2.6. Statistical analysis

Statistical analysis was performed using student *t*-test ($p \leq 0.05$). All results presented as the mean ± SD

3.3 Results

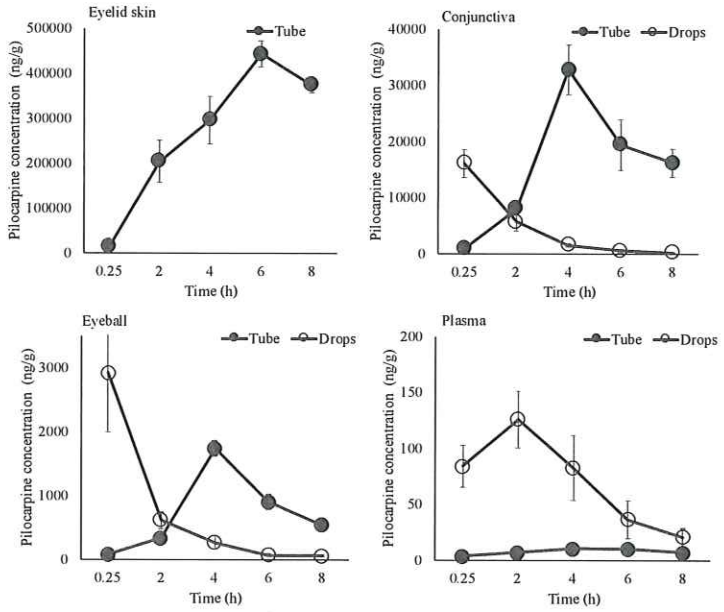

Concentration of pilocarpine in eyelid skin, conjunctiva, eyeball and plasma following topical eyelid and eyedrop administration.

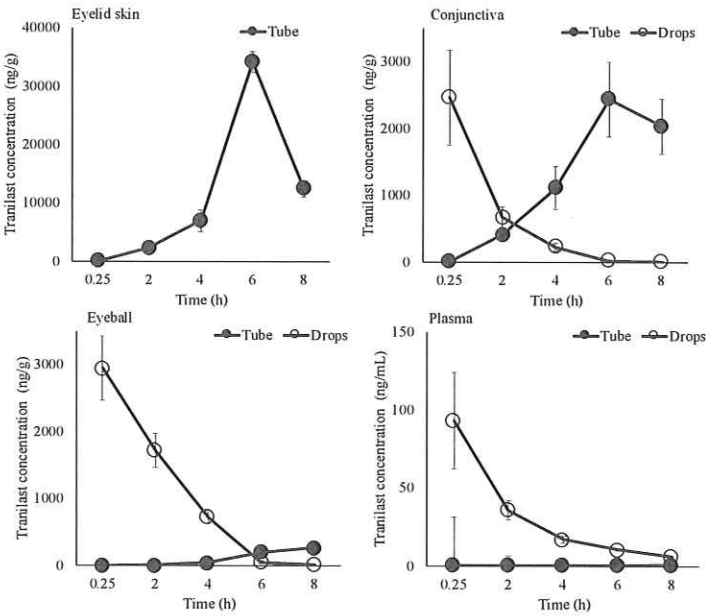

Concentration of tranilast in eyelid skin, conjunctiva, eyeball and plasma following topical eyelid and eyedrop administration.

References

Abd, E., Yousef, S.A., Pastore, M.N., Telaprolu, K., Mohammed, Y.H., Namjoshi, S., Grice, J.E., Roberts, M.S., 2016. Skin models for testing of transdermal drugs. Clin. Pharmacol. Adv. App. 8, 163-76.

Akhter, S., Anwar, M., Siddiqui, M.A., Ahmad, I., Ahmad, J., Ahmad, M.Z., Bhatnagar, A., Ahmad F.J., 2016. Improving the topical ocular pharmacokinetics of an immunosuppressant agent with mucoadhesive nanoemulsions: formulation development, in-vitro and in-vivo studies. Colloids and Surfaces B: Biointerfaces 148, 19 – 29.

Amirlak, B., Sahshabi, L., 2015. Skin Anatomy, http://emedicine.medscape.com/article/1294744-overview, (accessed 16. 05. 02).

Baranowski, P., Karolewicz, B., Gajada, M., Pluta, J., 2014. Ophthalmic drug dosage forms: characterisation and research methods. The Sci. World J. Article ID 861904. http://dx.doi.org/10.1155/2014/861904.

Chen, L., Han, L., Lian, G., 2013. Recent advances in predicting skin permeability of hydrophilic solutes. Adv. Drug Deliv. Rev. 65, 295 – 305.

Davies, N.M., 2000. Biopharmaceutical considerations in topical ocular drug delivery. Clin. Exp. Pharmacol. Physiol. 27, 558-562.

Desai, A., Lee, M. 2007. Gibaldi's drug delivery systems in pharmaceutical care. American Society of Health-System Pharmacists, Inc., Wisconsin Avenue, Bethseda, MD

Feingold, K.R., 2009. The outer frontier: the importance of lipid metabolism in the skin. J. Lipid. Res. 50, 417-422.

Gan, L., Han, S., Shen, J., Zhu, J., Zhu, C., Zhang, X., Gan, Y., 2010. Self-assembled liquid crystalline nanoparticles as a novel ophthalmic delivery system for dexamethasone: improving preocular retention and ocular bioavailability. Int. J. Pharm. 396, 179-187.

Gaudana, R., Ananthula, H.K., Parenky, A., Mitra, A.K., 2010. Ocular drug delivery. AAPS. J. 12, 348-360.

Gause, S., Hsu, K.H., Shafor, C., Dixon, P., Powell, K.C., Chauhan, A., 2016. Mechanistic modelling of ophthalmic drug delivery to the anterior chamber by eye drops and contact lenses. Adv. Colloid Interface Sci. 233, 139-154.

Hasegawa, T., Kawazome, A., Yanagimoto, G., Hayashi, T., Seki, T., Akimoto, M., Todo, H., Sugibayashi, K., 2007. Analysis of skin disposition of flurbiprofen after topical application using dual agar gel discs-inserted rats. Biol. Phar. Bull., 30, 2135-2140.

Isowaki, A., Ohtori, A., Matsuo, Y., Tojo, K., 2003. Drug delivery to the eye with a transdermal therapeutic system. Chem. Pharm. Bull. 26, 69-72.

Jung, E.C., Maibach, H.I., 2014. Animal models for percutaneous absorption, in: Shah, V., Maibach, H.I., Jenner, J. (Eds.), 2014. Topical Drug Bioavailability, Bioequivalence, and Penetration, Springer Science, New York, 21-30.

Kimura, C., Tojo, K., 2007. Development of a stick-type transdermal eyelid delivery system of ketotifen fumarate for ophthalmic diseases. Chem. Pharm. Bull. 55, 1002-1005.

Kumar, R., Sinha, V.R., 2016. Solid lipid nanoparticle: an efficient carrier for improved ocular permeation of voriconazole. Drug. Dev. Ind. Pharm. 42, 1956-1967.

Li, X., Nie, S.F., Kong, J., Li, N., Ju, C.Y., Pan, W.S., 2008. A controlled-release ocular delivery system for ibuprofen based on nanostructured lipid carriers, Int. J. Pharm. 363, 177-182.

Lux, A., Maier, S., Dinslage, S., Süverkrüp, R., Diestelhorst, M., 2003. A comparative bioavailability study of three conventional eye drops versus a single lyophilisate. Br. J. Ophthalmol. 87, 436-440.

Maistrello, I., Rigamonti, G., Frova, C., de Ruggieri, P., 1973. Quantitative effect of topically applied anti-inflammatory agents on external ocular inflammation in rats. J. Pharm. Sci. 62, 1455-1460.

Morimoto, Y., Hatanaka, T., Sugibayashi, K., Omiya, H., 1992. Prediction of skin permeability of drugs: comparison of human and hairless rat skin. J. Pharm. Pharmacol. 44, 634-639.

Pappas, A., 2009. Epidermal surface lipids. Dermatoendocrinol. 1, 72-76.

Paudel, K.S., Milewski, M., Swadley, C.L., Brogden, N.K., Ghosh, P., Stinchcomb, A.L., 2010. Challenges and opportunities in dermal/transdermal delivery. Ther. Deliv. 1, 109-131.

Pratchyapruit, W., Kikuchi, K., Gritiyarangasan, P., Aiba, S., Tagami, H., 2007. Functional analyses of the eyelid skin constituting the most soft and smooth area on the face: contribution of its remarkably large superficial corneocytes to effective water-holding capacity of the stratum corneum. Skin Res. Technol. 13, 169-175.

Potts, R.O., Guy, R.H., 1992. Predicting skin permeability. Pharm. Res. 9, 663 – 669.

Sheu, H.M., Tsai, J.C., Lin, T.K., Wong, T.W., Lee, J.Y., 2003. Modified Nile red staining method for improved visualization of neutral lipid depositions in stratum corneum. J. Formos. Med. Assoc. 102, 656-660.

Sugibayashi, K., Yanagimoto, G., Hayashi, T., Seki, T., Juni, K., Morimoto, Y., 1999, Analysis of skin disposition of flurbiprofen after topical application in hairless rats. J. Control. Release 62, 193-200.

Sugibayashi, K., Todo, H., Oshizaka, T., Owada, Y., 2010. Mathematical model to predict skin concentration of drugs: toward utilization of silicone membrane to predict skin concentration of drugs as an animal testing alternative. Pharm. Res. 27, 134-142.

Wang, S., Zhang, J., Jiang, T., Zheng, L., Wang, Z., Zhang, J., Yu, P., 2011. Protective effect of coenzyme Q_{10} against oxidative damage in human lens epithelial cells by novel ocular drug carriers. Int. J. Pharm. 403, 219 – 229.

Watanabe, T., Hasegawa, T., Takahashi, H., Ishibashi, T., Takayama, K., Sugibayashi, K., 2011. Utility of three-dimensional cultured human skin model as a tool to evaluate skin permeation of drugs. Altern. Animal Test Experiment. 8, 1-14.

Ya-Xian, Z., Suetake, T., Tagami, H., 1999. Number of cell layers of the stratum corneum in normal skin - relationship to the anatomical location on the body, age, sex and physical parameters. Arch. Dermatol. Res. 291, 555-559.

Chapter 2 References

1. Arroyo, C.M., Quinteros, D., Cozar-Bernal, M.J., Palma, S.D., Rabasco, A.M., Gonzales-Rodriguez, M.L., 2018. Ophthalmic administration of a 10-fold-lower dose of conventional nanoliposome formulations caused levels of intraocular pressure similar to those induced by marketed eye drops. Eur. J. Pharm. Sci. 111, 186 – 194.
2. Rupenthal, D., 2017. Drug-device combination approaches for delivery to the eye. Curr. Opin. Pharmacol. 36, 44 – 51.
3. See, G.L., Sagesaka, A., Sugasawa, S., Todo, H., Sugibayashi, K., 2017. Eyelid skin as a potential site for drug delivery to conjunctiva and ocular tissues. Int. J. Pharm. 533, 198 – 205.
4. Gause, S., Hsu, K.H., Shafor, C., Dixon, P., Powell, K.C., Chauhan, A., 2016. Mechanistic modelling of ophthalmic drug delivery to the anterior chamber by eye drops and contact lenses. Adv. Colloid Interface Sci. 233, 139 – 154.
5. Januleviciene, I., Siaudvytyte, L., Barsauskaite, R., 2012. Ophthalmic drug delivery in glaucoma – a review. Pharmaceutics. 4, 243 – 251.
6. Janagam, D.R., Wu, L., Lowe, T.L., 2017. Nanoparticles for drug delivery to the anterior segment of the eye. Adv. Drug Deliv. Rev.122, 31 – 64.

7. Baranowski, P., Karolewicz, B., Gajada, M., Pluta, J., 2014. Ophthalmic drug dosage forms: characterisation and research methods. The Sci. World J. Article ID 861904.
8. Kimura, C., Tojo, K., 2007. Development of a stick-type transdermal eyelid delivery system of ketotifen fumarate for ophthalmic diseases. Chem. Pharm. Bull. 55, 1002-1005.
9. Isowaki, A., Ohtori, A., Matsuo, Y., Tojo, K., 2003. Drug delivery to the eye with a transdermal therapeutic system. Chem. Pharm. Bull. 26, 69-72.
10. Pratchyapruit, W., Kikuchi, K., Gritiyarangasan, P., Aiba, S., Tagami, H., 2007. Functional analyses of the eyelid skin constituting the most soft and smooth area on the face: contribution of its remarkably large superficial corneocytes to effective water-holding capacity of the stratum corneum. Skin Res. Technol. 13, 169-175.
11. Huang, D., Chen, Y.S., Rupenthal, I.D., 2017. Overcoming ocular drug delivery barriers through the use of physical forces. Adv. Drug Deliv. Rev.
12. Eljarrat-Binstock, E., Domb, A.J., 2006. Iontophoresis: a non-invasive ocular drug delivery. J. Controlled Release. 110, 479 – 489.
13. Maistrello, I., Rigamonti, G., Frova, C., de Ruggieri, P., 1973. Quantitative effect of topically applied anti-inflammatory agents on external ocular inflammation in rats. J. Pharm. Sci. 62, 1455-1460.
14. Bertens, C.J.F., Gijs, M., van der Biggelaar, F.J.H.M., Nuijts, R.M.M.A., 2018. Topical drug delivery devices: a review. Exp. Eye Res. 168, 149 – 160.
15. Watanabe, T., Hasegawa, T., Takahashi, H., Ishibashi, T., Takayama, K., Sugibayashi, K., 2011. Utility of three-dimensional cultured human skin model as a tool to evaluate skin permeation of drugs. Altern. Animal Test Experiment. 8, 1-14.
16. Morimoto, Y., Hatanaka, T., Sugibayashi, K., Omiya, H., 1992. Prediction of skin permeability of drugs: comparison of human and hairless rat skin. J. Pharm. Pharmacol. 44, 634-639.
17. Zhang, Y., Chen, Y., Yu, X., Yangjia, Qi., Chen, Y., Liu, Y., Hu, Y., Li, Z. 2016. A flexible device for ocular iontophoretic drug delivery. Biomicrofluidics 10, 011911
18. Gomez, C. C. S., Servidoni, M. de F., Marson, F. A. de L., Canavezi, P. J. C., Vinagre, A. M., Costa, E. T., … Ribeiro, J. D., 2014. Pulsed direct and constant direct currents in the pilocarpine iontophoresis sweat chloride test. BMC Pulmonary Medicine 14, 198.

19. Birmingham, A.T., Galloway, N.R., Walker, D.A., 1979. Intraocular pressure reduction in chronic simple glaucoma by continuous infusion of dilute pilocarpine solution. Br. J. Ophthalmol. 63, 808 – 812.
20. Schmidl, D., Schmetterer, L., Garhöfer, G., Popa-Cherecheanu, A., 2015. Pharmacotherapy of glaucoma. J. Ocul. Pharmacol. Ther. 31, 63 – 77.
21. Hosoya, K., Lee, V.H.L., Kim, K.J., 2005. Roles of conjunctiva in ocular drug delivery: a review of conjunctival transport mechanisms and their regulation. Eur. J. Pharm. Biopharm. 60, 227 – 240.
22. Sasaki, H., Yamamura, K., Nishida, K., Nakamura, J., Ichikawa, M. 1996. Delivery of drugs to the eye by topical application. Progress in Retinal and Eye Res. 15, 583 – 620.
23. Pilocarpine hydrochloride, 2009. https://www.fda.gov/downloads/Drugs/DevelopmentApprovalProcess/DevelopmentResources/UCM218910.pdf (accessed 01 January 2018).
24. Davis, J.L., Gilger, B.C., Robinson, M.R. 2004. Novel approaches to ocular drug delivery. Curr. Opin. Mol. Ther. 6, 195 – 205.
25. Nasir, N.A.A., Agarwal, P., Agarwal, R., Iezhitsa, I., Alyautdin, R., Nukolova, N.N., Chekhonin, V.P., Ismail, N.M. 2017. Intraocular distribution of topically applied hydrophilic and lipophilic substances in rat eyes. Drug Deliv. 23, 2765 – 2771.
26. Chien, D.S., Homsy, J.J., Gluchowski, C., Tang-Liu, D.D.S. 1990. Corneal and conjunctival/scleral penetration of p-aminoclonidine, AGN 190342, and clonidine in rabbit eyes. Curr. Eye Res. 9, 1051 – 1059.